

# Fretting behaviour of 316L stainless steel produced by powder injection moulding

H. I. Bakan<sup>1\*</sup>, J. P. Celis<sup>2</sup>

<sup>1</sup>*TUBITAK MAM Materials Institute, P.O. Box 21, Gebze 41470, Kocaeli, Turkey*

<sup>2</sup>*Katholieke Universiteit Leuven, Department of Metallurgy and Materials Engineering (MTM), Kasteelpark Arenberg 44, B-3001 Leuven, Belgium*

Received 6 December 2010, received in revised form 20 April 2011, accepted 21 April 2011

## Abstract

The biocompatible metals made available for powder injection moulding (PIM) are increasing, and as a result, the PIM process is becoming attractive for manufacturers of medical implants and surgical instruments. In addition, friction and wear properties play an important role in biomaterial applications. This study aimed to systematically investigate the fretting wear properties of 316L stainless steel parts produced by PIM under dry contact conditions. The fretting experiments were performed under gross-slip regime. The influence of a number of fretting test parameters on the friction and wear behaviour was investigated, as the contact frequency, the normal load, and number of reciprocating sliding cycles. Fretting tests were performed against corundum counter bodies. After the tests, the wear scars were examined by laser surface profilometry, scanning electron microscopy (SEM) and energy dispersive X-ray microanalysis. The results indicate that wear occurred predominantly by abrasion, plastic deformation, and cracking.

**Key words:** fretting, stainless steel, powder injection moulding, biomaterials

## 1. Introduction

Fretting is a wear phenomenon occurring when two contacting solids are subjected to a relative oscillatory tangential motion of small displacement amplitude. This small oscillatory displacement along the contact interface can result in the renewal of material by wear or the initiation of cracks by cyclic contact stresses. Fretting conditions are found in virtually any technical system where contact vibrations are induced by cyclic accelerations, fatigue stresses, acoustical noise, or temperature variations. It is known that even displacement amplitudes in the sub-micron range can result in wear damage. Fretting becomes an important aspect to designers when the functionality of a component deteriorates or its lifetime is reduced by the induced material damage. Fretting may occur at the interface between a prosthetic device and human organ and within the assemblies of a single prosthetic device. Typical fretting cases in clinical practice can be observed at screw-plate interfaces, artificial hip joint-

-bone interfaces and residual human limb-artificial limb joint interfaces. In addition, failures of tooth implants are frequently observed in clinical practice at the interfaces between screw, tooth crown and alveolar bone, essentially induced during mastication [1–5].

Powder injection moulding (PIM) is a manufacturing process commonly used for medical devices, especially implants and instruments made of difficult-to-machine materials such as stainless steels and titanium alloys [6–8]. Type 316L stainless steel has been widely used for many implant applications such as bones, plates, screws, staples, pins, and nail stents. Surgical instruments are generally produced from stainless steels because of the strength, hardness, corrosion resistance, and ease of sterilization of these materials. PIM combines the process ability of plastics and the superior material properties of metals to form high performance components. PIM is composed of several processes: fine powders are mixed with binders in order to get the feedstock, the feedstock is injected into a mould, binders are removed from the injection-

\*Corresponding author: tel.: +90 262 6773037; fax: +90 262 6412309; e-mail address: [Halil.Bakan@mam.gov.tr](mailto:Halil.Bakan@mam.gov.tr)

Table 1. Physical and mechanical properties of 316L stainless steel specimens produced by PIM in comparison with wrought 316L stainless steel [11]

	Density	Hardness	Yield strength	Tensile strength	Elongation
PIM 316L	$7.88 \text{ g cm}^{-3} \pm 0.02$	$80 \text{ HRB} \pm 0.7$	$182 \text{ MPa} \pm 1.7$	$485 \text{ MPa} \pm 3.3$	$40 \% \pm 2.50$
Wrought 316L	$7.9 \text{ g cm}^{-3}$	$< 92 \text{ HRB}$	$> 170 \text{ MPa}$	$> 480 \text{ MPa}$	$> 30 \%$

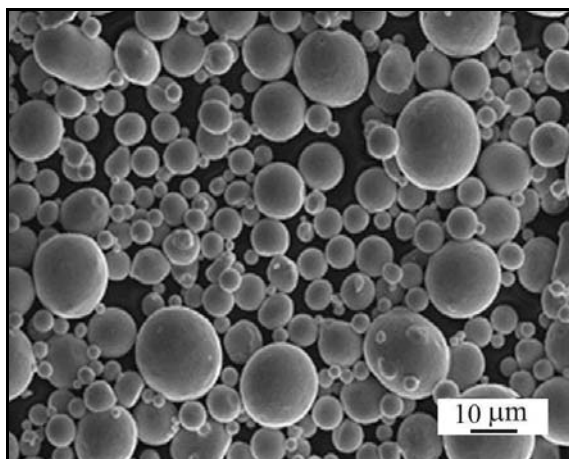


Fig. 1. Scanning electron micrograph of gas atomised 316L powder.

-moulded body and then only powders are sintered at high temperatures. The important benefits of PIM include near net-shape production of complex geometries in the context of low cost and rapid fabrication at high production volumes [9].

It is assumed that the wear resistance of PIM parts is one of most important properties since surface characteristics are factors determining the lifetime of various PIM parts used for biomedical purposes. Despite the fact that PIM parts have become popular in recent years, the fretting behaviour of metallic parts produced by PIM has not been studied yet. The objective of this research was to investigate the fretting wear behaviour of 316L stainless steel produced by PIM under dry sliding against a corundum ball.

## 2. Experimental studies

### 2.1. Materials and test pieces preparations

The powder used was gas atomised 316L austenitic steel with a mean particle size of  $16 \mu\text{m}$  (Fig. 1). The chemical composition of the powder was Fe-16.96, Cr-10.8, Ni-2.04, Mo-1.38, Mn-0.45, Si-0.03, C-0.03, P-0.003 and S (wt.%). Nickel boride (NiB) powder with a mean particle size of  $25 \mu\text{m}$  was used as a liquid phase sintering additive to achieve full densification [10]. For injection moulding, the feedstock contain-

ing 60 vol.% of 316L powder with 1.5 wt.% NiB was prepared by mixing the powders with a paraffin wax-polypropylene-based binder system for 30 min with a sigma blade mixer operated at  $125^\circ\text{C}$ . After cooling, the feedstock was pelletized using a granulator. This feedstock was injected into a mould of tensile test bars using a plunger type injection moulding machine at a pressure of 40 MPa. The nozzle and the mould temperatures were kept at  $165$  and  $23^\circ\text{C}$ , respectively. Debinding of injection moulded green parts was performed in two steps. Initial debinding was carried out in heptanes at  $60^\circ\text{C}$  for 4 h. This was followed by a thermal debinding and pre-sintering in a hydrogen atmosphere. For thermal debinding, specimens were heated at a rate of  $2^\circ\text{C min}^{-1}$  up to  $450^\circ\text{C}$ , and held for 90 min. This was followed by a  $5^\circ\text{C min}^{-1}$  heating up to  $1000^\circ\text{C}$  that was kept for 60 min as pre-sintering step, followed by a furnace cooling down to room temperature at a rate of  $5^\circ\text{C min}^{-1}$ . A set point of  $1000^\circ\text{C}$  was used to impart handling strength. Sintering was carried out in vacuum at a base pressure of 4 Pa. The parts were placed on alumina trays and heated up to  $1000^\circ\text{C}$  at a rate of  $10^\circ\text{C min}^{-1}$ , and kept at that temperature for 10 min. Then the parts were heated at  $5^\circ\text{C min}^{-1}$  up to the sintering temperature of  $1285^\circ\text{C}$ , kept at this temperature for 90 min, and finally cooled down to room temperature at a rate of  $10^\circ\text{C min}^{-1}$ . The density of the sintered samples was  $7.88 \text{ g cm}^{-3}$  as measured by Archimedes' principle. The Rockwell B hardness and tensile strength of the sintered samples were 80 HRB and 485 MPa, respectively. Mechanical properties of the sintered samples are very competitive with wrought materials, as appears from Table 1 [11]. These properties are sufficient to meet the requirements for medical instruments as given in ASTM F899-95.

For metallographic examination by optical and scanning electron microscopy, sintered samples were polished using standard metallographic techniques and electrolytic etching in oxalic acid. The sintered samples have a relatively homogeneous microstructure (Fig. 2).

### 2.2. Fretting wear testing

The fretting wear tests were performed with a computer-controlled fretting simulator, described in the previous study [12]. Wear was achieved by sliding

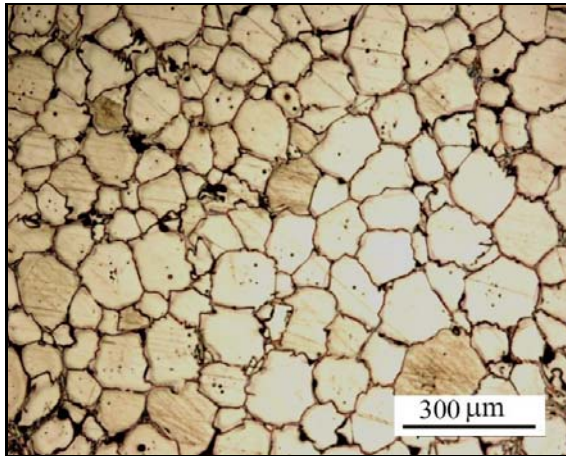


Fig. 2. Optical micrograph of stainless steel after sintering at 1285°C for 90 min.

against a polycrystalline corundum ball (Cerotec, Geldermalsen, The Netherlands). The motion consisted of a reciprocating oscillation under small displacement amplitude sliding. The corundum balls used as sliding counter bodies had a diameter of 10 mm, Vickers hardness of 2000 HV, and a surface roughness of 0.02  $\mu\text{m}$  ( $R_a$ ). Test samples were cut from the sintered 316L tensile test bar specimen into cylindrical pieces with a diameter of 25 mm and thickness of 4 mm by using a diamond cutting machine.

Prior to the fretting tests, the flat part of the cylindrical pieces was polished with diamond paste, and subsequently with a colloidal solution of silica until an average surface roughness  $R_a = 0.1 \mu\text{m}$  was obtained. Polished 316L pieces and corundum counter bodies were degreased with acetone and ethanol (naturalised ethanol and 5 percent diethyl ether) to remove oils and other contaminants, then rinsed with deionised water, and finally dried in hot air. Fretting tests were performed at 23°C in ambient air of 50 % relative humidity (RH). Surface morphology of wear tracks was examined by scanning electron microscopy and laser profilometry (WYKO NT 3300). EDAX analyses were done at an acceleration voltage of 5 kV.

### 3. Results and discussion

The maximum tangential force recorded after different numbers of fretting cycles performed at 5 N applied normal load is shown in Fig. 3 for reciprocating sliding tests done for different fretting frequencies. During the “running-in” period that lasts over the first 500 cycles, the maximum tangential force increases from 4.0 up to 4.6 N at a fretting frequency of 10 Hz, from 3.7 up to 4.4 N at 5 Hz, and from 3.3 up to 4.4 N at 1 Hz fretting frequency. Once the maximum tangential force is reached, the tangential force

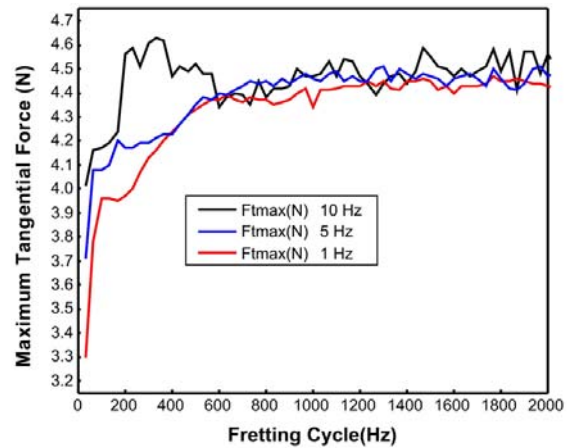


Fig. 3. Influence of the contact frequency on the tangential force recorded on 316L stainless steel produced by PIM and sliding against corundum at 5 N load, 100  $\mu\text{m}$  displacement, amplitude for tests performed in ambient air of 50 % relative humidity and 23°C.

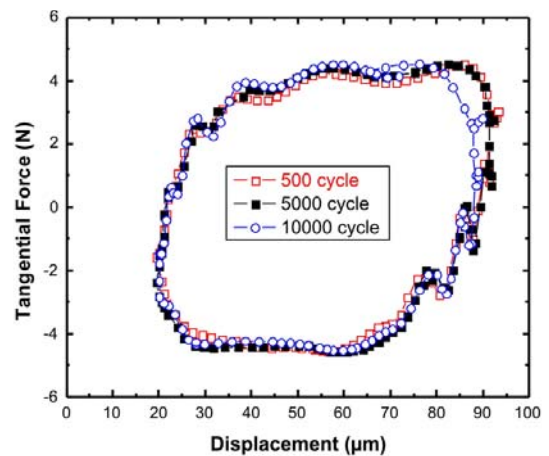


Fig. 4. Typical fretting hysteresis loops recorded on 316L stainless steel produced by PIM sliding against corundum at 5 N normal load, 10 Hz, 100  $\mu\text{m}$  displacement amplitude for dry sliding tests performed in ambient air of 50 % relative humidity and 23°C.

becomes rather stable, and a relatively steady state is noticed during the subsequent fretting cycles.

Typical tangential force-displacement hysteresis loops (known as fretting loops) are shown in Fig. 4 for different numbers of fretting cycles. The area of these hysteresis loops corresponds to the friction energy dissipated during each fretting cycle. Once the running-in is completed, the frictional tangential force remains fairly constant during subsequent fretting cycles, and the shape of the hysteresis loops indicates that a gross slip fretting regime is prevailing. These results correspond to test data shown in Fig. 3.

Figure 5 shows the variation of the dissipated en-

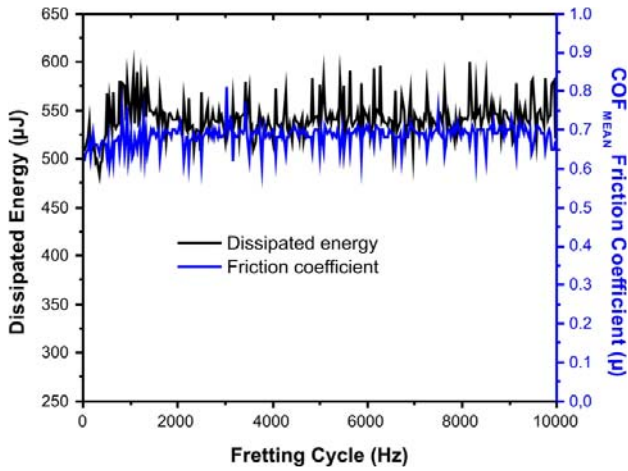


Fig. 5. Variation of dissipated energy and coefficient of friction with the number of fretting cycles during fretting tests performed in ambient air ( $F_N$ : 5 N, displacement: 100 μm, contact frequency: 10 Hz) on 316L stainless steel produced by PIM sliding against corundum.

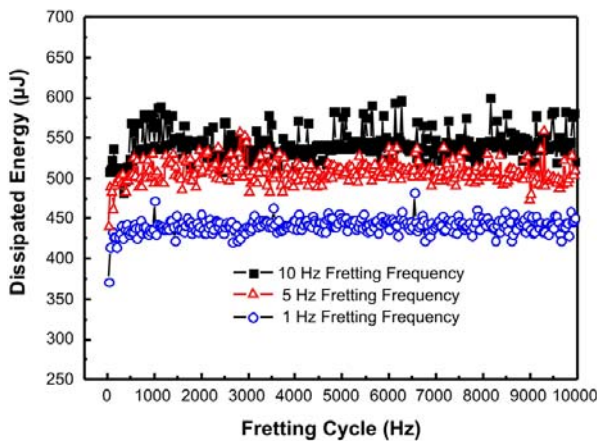


Fig. 6. Influence of the contact frequency on the dissipated energy recorded on PIM 316L stainless steel sliding against corundum at 5 N normal load, 100 μm displacement amplitude, during dry tests performed in ambient air of 50 % relative humidity at 23°C.

ergy and the coefficient of friction with the number of fretting cycles. The dissipated energy is independent of the number of fretting cycles once the running-in is completed. The dissipated energy increases with increasing fretting frequency as can be seen from Fig. 6. Also the coefficient of friction is relatively stable, and is about 0.68.

The wear volume is shown respectively in Fig. 7a,b for tests performed at different fretting frequency and fretting load. The increase in frequency from 1 to 10 Hz causes a slight increase in wear volume from 18000 to 24000 μm<sup>3</sup>. The wear volume increases in a more pronounced way from 12000 to 24000 μm<sup>3</sup> at

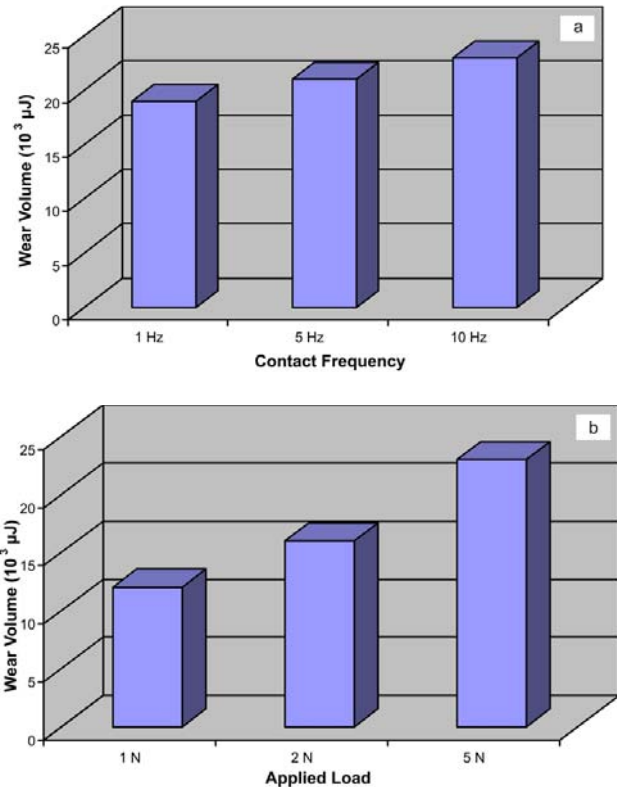


Fig. 7. Wear volume recorded on PIM 316L stainless steel after fretting tests performed in ambient air of 50 % relative humidity at 23°C: a) at contact frequency and b) at varying normal load.

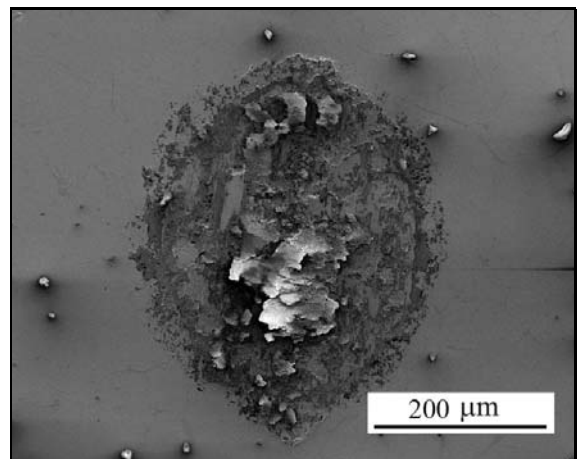


Fig. 8. Morphology of wear scar on PIM 316L stainless steel after a fretting test performed against corundum at 10 Hz contact frequency in air of 50 % RH and 23°C for 10000 cycles at 5 N normal load and 100 μm displacement amplitude.

increasing normal load from 1 to 5 N.

SEM micrograph of fretting wear scars on PIM 316L stainless steel after 10000 fretting cycles in am-

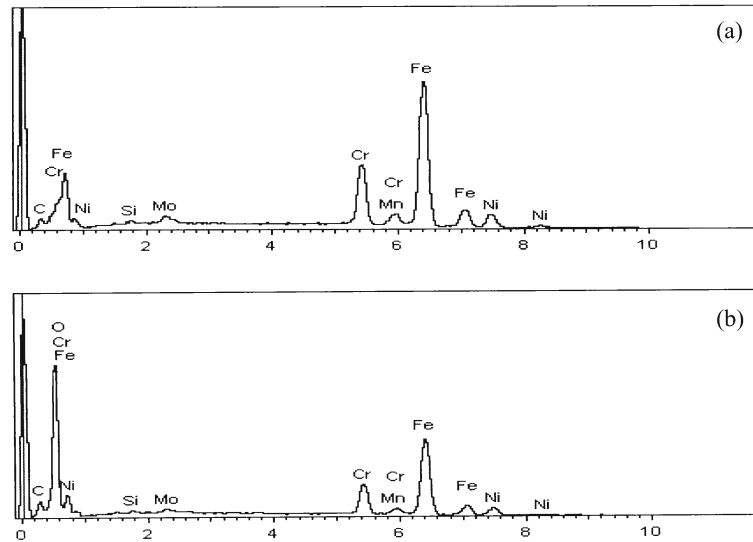


Fig. 9. EDAX results of PIM 316L for a) original surface and b) wear trace of the surfaces loaded at 5 N for 10000 cycles.

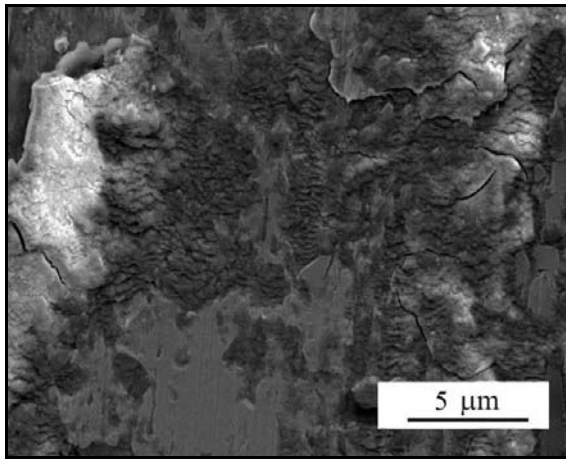


Fig. 10. Details of the morphology of wear scars on PIM 316L stainless steel after sliding tests performed against corundum at 10 Hz contact frequency in air of 50 % RH for 10000 cycles at 5 N normal load and 100  $\mu\text{m}$  displacement amplitude.

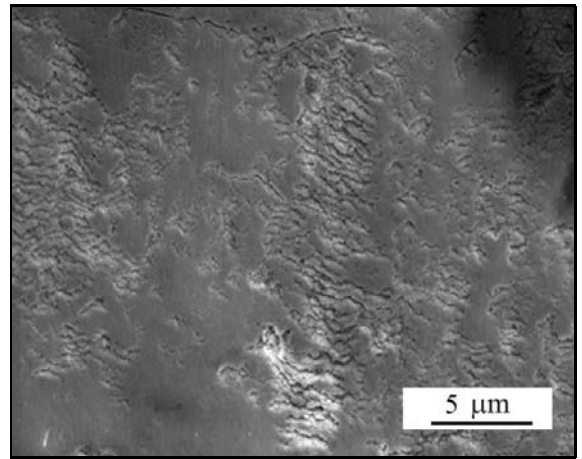


Fig. 11. Detail of the morphology of the wear scar on PIM 316L stainless steel after fretting test performed against corundum for 300 fretting cycles in ambient air of 50 % RH at 23°C, at 5 N normal load, 10 Hz, and 100  $\mu\text{m}$  displacement amplitude.

bient air is shown in Fig. 8. All wear scars are elliptic with the longer axis parallel to the sliding direction and covered with a surface layer containing fine cracks. EDAX analysis revealed a relatively high content of iron, chromium and oxygen in these wear tracks in comparison with the original materials (Fig. 9). Outside the wear tracks, delaminated surface layers are visible, as well as ejected wear debris that formed agglomerated particles. In addition, scratches parallel to the sliding direction are present (Fig. 10). Such scratches are typical of abrasive wear. Wear scars are characterized by the presence of deep abrasive scratches, the pile up of debris, and some cracks. The cracks are oriented both perpendicular and parallel to the abrasive scratches. In

the worn area, high plastic deformation is clearly visible.

At the end of the running-in period that lasts for about 100 sliding cycles, a few scratches were observed in the wear scar on PIM 316L stainless steel (Fig. 11). After 300 sliding cycles, EDAX analyses did not reveal any substantial amount of oxygen in the wear tracks. However after 1000, 5000, and 10000 fretting cycles, relatively high contents of oxygen were detected in the wear tracks. The amount of oxygen in the wear track increased with the number of fretting cycles, suggesting the progressive formation of an oxide film. As a result, the wear process evolves from a mild abrasive wear into an oxidational wear with increasing number of fretting cycles.

#### 4. Conclusions

The fretting wear behaviour of 316L stainless steel parts produced by PIM was investigated by performing fretting tests under gross slip contact conditions. Their mechanical properties are very competitive with the ones of wrought materials, and are sufficient to meet the requirements for medical instruments. Flat PIM 316L samples were subjected to contact vibrations against corundum balls during tests performed in ambient air of medium relative humidity ( $RH \approx 50\%$ ) under gross slip regime. A detailed microstructural investigation of the worn surface by SEM suggests that the major wear mechanisms active on 316L stainless steel produced by PIM are abrasion, debris formation, and cracking.

#### Acknowledgement

Dr. Halil I. Bakan acknowledges TUBITAK MAM (The Scientific and Technological Research Council of Turkey, Marmara Research Centre) for the financial support allowing him to perform research at the Katholieke Universiteit Leuven, Dept. MTM, B-3001 Leuven (Belgium).

#### References

- [1] HOEPPNER, D. W.—CHANDRASEKARAN, V.: *Wear*, 173, 1994, p. 189.  
[doi:10.1016/0043-1648\(94\)90272-0](https://doi.org/10.1016/0043-1648(94)90272-0)
- [2] RAMALHO, A.—CELIS, J. P.: *Tribol. Lett.*, 14, 2003, p. 187. [doi:10.1023/A:1022368414455](https://doi.org/10.1023/A:1022368414455)
- [3] ZHU, M. H.—CAI, Z. B.—LI, W.—YU, H. Y.—ZHOU, Z. R.: *Tribol. Int.*, 42, 2009, p. 1360.  
[doi:10.1016/j.triboint.2009.04.007](https://doi.org/10.1016/j.triboint.2009.04.007)
- [4] RYBIAK, R.—FOUVRY, S.—BONNET, B.: *Wear*, 268, 2010, p. 413.
- [5] CRUZADO, A.—HARTELT, M.—WASCHE, R.—URCHEGUI, M. A.—GOMEZ, X.: *Wear*, 268, 2010, p. 1409.
- [6] JOHNSON, J. L.—HEANEY, D. F.: *Medical Device Materials II: 2005*, p. 325.
- [7] GERMAN, R. M.: *Int. J. Powder Metall.*, 36, 2000, p. 31.
- [8] TOMLIN, T. A.: *Int. J. Powder Metall.*, 36, 2000, p. 53.
- [9] GERMAN, R. M.—BOSE, A.: *Injection Moulding of Metal and Ceramic*. Princeton, NJ, MPIF 1997.
- [10] BAKAN, H. I.—HEANEY, D. F.—GERMAN, R. M.: *Powder Metall.*, 44, 2001, p. 235.  
[doi:10.1179/003258901666392](https://doi.org/10.1179/003258901666392)
- [11] DAVIS, J. R., Ed.: *ASM Specialty Handbook: Stainless Steels*. Materials Park, Ohio, ASM International 1994.
- [12] MOHRBACHER, H.—CELIS, J. P.—ROOS, J. R.: *Tribol. Int.*, 2, 1995, p. 269.